
QUANTIFYING BARRIERS OF URBAN MOBILITY

A PREPRINT

Gergő Pintér ^{1,2,*} and Balázs Lengyel ^{1,2,3,4}

¹ANETI Lab, Corvinus University of Budapest, Budapest, 1093, Hungary and HUN-REN Centre for Economic and Regional Studies, Budapest, 1097, Hungary

²Corvinus Institute for Advanced Studies, Corvinus University of Budapest, Budapest, 1093, Hungary

³Institute of Economics, HUN-REN Centre for Economic and Regional Studies, Budapest, 1097, Hungary

⁴Institute for Data Analytics and Information Systems, Corvinus University of Budapest, Budapest, 1093, Hungary

*Corresponding author: gergo.pinter@uni-corvinus.hu

August 29, 2024

ABSTRACT

Barriers in cities, such as administrative boundaries, natural obstacles, railways or major roads are thought to induce segregation. However, the empirical knowledge about this phenomenon is limited. Here, we present a network science framework to assess barriers to urban mobility along their hierarchy, across residential areas and visited amenities. Using GPS mobility data, we construct a network of blocks from the sequence of individual stays in a major European city. A community detection algorithm allows us to partition this network into non-overlapping areas of dense mobility clusters, in which the effect of transportation hubs can be tuned with a parameter. We apply the Symmetric Area Difference index to quantify the overlap between these mobility clusters and the polygons of urban area separated by barriers. Reducing the effect of transportation hubs results in smaller scale mobility clusters that fit better to lower rank administrative or road barriers compared to their higher rank pairs. We find that characteristic urban barriers can replace each other in dividing mobility clusters of different scales. Next, we define the Barrier Crossing Ratio, the fraction of barrier crossings that bridge mobility clusters. The decomposition of this indicator by origins and destinations suggests a significantly higher impact of barriers on those who live closer to the city center and smaller impact on visits to complex amenities. These results contribute to the ongoing discourse on urban segregation, emphasizing the importance of barriers to urban mobility in shaping interactions and mixing.

Introduction

Mixing people is essential for cities' economic progress; yet, most interaction happen within neighborhoods [1]. Residential segregation is known to worsen economic opportunities and health outcomes of the poor [2, 3], is associated with high crime levels [4], and has been found to hinder economic growth of cities [5]. Building on recent developments in urban mobility research that leverages high resolution location data retrieved from mobile devices [6, 7, 8], segregation inquiry is increasingly moving to understand mixing beyond residential areas. This literature has documented in detail that social mixing varies by locations and amenities in the city [9, 10, 11, 12, 13, 14] and is influenced by mobility policies [15, 16]. However, the role of urban barriers, despite their direct impact on mobility [17], has remained an unsolved puzzle.

Major roads are great examples of this puzzle, as these were built to increase accessibility, but roads connecting distant places can be obstacles for local mobility [18]. Research in "Road Ecology" investigates the impact of roads on wildlife [19], and has led to different types of mitigation measures in the last decades to reduce the number of roadkill, including building tunnels and bridges for mammals [20] or amphibians [21]. The barrier effect (also known as "community severance") is also examined in human environments, but are mainly conducted via surveys [22, 23, 18] and focus on a specific part of a city [24, 18]. Further characteristic physical barriers like railways, parks or rivers

are natural borders between neighborhoods [25] and can amplify segregation by hindering mixing and interaction across separated areas [26, 27, 28]. However, the questions of which barriers limits mixing, where in the city and for whom, have not been answered.

In this paper, we contribute a network science framework to evaluate the role of barriers in urban mobility. The basis of the approach is a widely used community detection procedure that, in our case, groups together locations by maximizing the density of mobility flows within groups [29, 30]. Compared to other approaches that evaluate barriers by quantifying the probability of mobility for pairs of locations, community detection reveals clustering relationships among locations acknowledging that individuals often are present in more than two locations during the day and their mobility flows contains more than one network edge [17]. Community detection on spatial networks can reveal the role of barriers by analyzing how clusters of such complex mobility flows fit to these boundaries. The method can be fine-tuned to decrease the impact of large mobility hubs and increase the importance of local mobility flows that can help find the scales of clustered mobility links that have the best fit to urban barriers [7, 31].

The method is demonstrated with an empirical exercise based on a GPS mobility data set that contains 161,294 mobile phone devices in Budapest, Hungary over 6 months before and 6 months during the COVID-19 pandemic. From the geolocation and time-stamp of pings, we construct a mobility network, in which nodes are blocks where individuals spent at least 15 minutes and edges are weighted by the number of individual mobility events between the blocks during the day. We first assess the role of various administrative and physical barriers as obstacles to mobility with a gravity model. Next, we run the Louvain community detection algorithm [29] on the mobility network that helps us identify dense mobility clusters. By increasing the resolution parameter of the algorithm, we mitigate the dominance of mobility hubs and group blocks into clusters of relatively smaller sizes. Then, we identify polygons of residential areas bounded by characteristic barriers and calculate the Symmetric Area Difference (SAD) indicator that is a global indicator to quantify how mobility clusters align with boundaries. Finally, we compute the Barrier Crossing Ratio (BCR) to capture the relationship between mobility events across urban barriers and detected mobility clusters that can be decomposed by origins and destinations. This procedure and the novel indicators enable us to quantify the impact of urban barriers on mobility across the hierarchies of barriers, across residential locations and visited amenities.

We find that administrative barriers, rivers, and roads significantly decrease mobility but their impact varies across the city. Increasing the resolution parameter, we observe an improved alignment – measured by the SAD indicator – with lower rank administrative barriers and secondary roads, while the fit with higher rank administrative boundaries and major roads improves only up to a certain point. We demonstrate that this is due to a shift among barrier as we mitigate the role of transportation hubs, characteristics urban barriers replace each other in dividing mobility clusters. Next, we decompose the BCR indicator by home locations and find that the impact of barriers depends on the residential areas and visited amenity locations. Mobility clusters of urban dwellers fit to all barriers significantly better than the mobility of residents who commute to the city from its agglomeration suggesting that barriers have a higher effect on local mobility than on those that link distant places. The measure also implies that barriers are not likely to impact mobility to amenities that are rarely found elsewhere in the city, except the river that is the most significant boundary of mobility. Repeating the exercise for Nagoya, Japan using a distinct data set, we find that fitting the mobility clusters to higher versus lower level urban barriers can reveal general patterns across cities. However, the method is also able to show differences that we show by contrasting barrier impact by home location.

Results

Empirical framework

Our GPS mobility data contains 135,271 devices in Budapest that we aggregate to a 6 months period starting from September 2019 and 35,894 devices that are aggregated to 6 months time window starting from November 2020 that contains the second and third waves of COVID-19 contagions in Hungary (see Figure S1 of the Supplementary Section S1). The data consist of the location coordinates and time stamp of pings generated by mobile apps. The analysis is restricted to those mobile phones that have at least 20 pings, similarly to [12]. Then, we construct a mobility network that connects blocks across the city following two steps. First, we identify blocks where individuals spend at least 15 minutes by a stop-detection algorithm [32] that clusters the ping sequences of single mobile phones in space and time [12]. Second, we link those blocks that individuals visit subsequently during the day and generate a network in which the edge weight is the number of individual mobility flows over a 6-month period, either before the COVID-19 pandemic (see a representation of this network in Figure 1a) or during the COVID-19 restrictions. Next, we identify home location of every phone as the most frequently visited stop in the evening and during nighttime. A home is identified for the entire period only if it appears to be home for at least 10 days. Finally, to capture barriers, we apply the openly available OpenStreetMap data for Budapest that contains polygons of rivers, railroads, and hierarchies of

administrative boundaries and roads (Figure 1d). Details of mobility and urban barrier data, the cleaning process, and the network generation procedure are explained in Materials and Methods.

Previous research investigated the impact of barriers on days of mobility links [17]. This approach has limitations in capturing the full complexity of mobility networks that can be important since mobility during the day typically include more stops that can form triangles, and more complex patterns. Here, we apply a widely used community detection method on the mobility network that can provide new insights by detecting dense mobility clusters that contain most of the mobility events and can represent silos of highly likely mobility links. We use the Louvain algorithm [29] that partitions nodes by maximizing the modularity index that is calculated using the formula (Eq. 1).

$$Q = \frac{1}{2m} \sum_{ij} \left[A_{ij} - \gamma \frac{k_i k_j}{2m} \right] \delta(c_i, c_j), \quad (1)$$

where A_{ij} is the weight of the link between block i and j , k_i is the sum of the weights of links of block i , c_i and c_j denote the community of blocks i and j , δ is equal to 1 if $c_i = c_j$ and zero otherwise and m is the sum of the weights in the network. Increasing the resolution parameter $\gamma > 0$, one can get smaller communities, while a small γ provides large communities. In our mobility network, this procedure mitigates the role of flows between large mobility hubs and enables the emergence of local mobility clusters. Previous research has shown that community detection on spatial networks forms spatially segregated partitions [31, 33, 34, 35] and increasing the resolution parameter has been applied to partition labor mobility networks into occupations with similar skill requirements [36] and also to find the scale of administrative boundaries that fragment commuting networks across cities [37].

However, detecting the role of barriers in urban mobility networks requires further analyzes, since a variety of boundaries may hinder mobility and thus partition the network, while their impact may differ across the city in non-trivial ways. In our Budapest case, for example, administrative barriers define communities in the Northeastern part of the city where major roads have seemingly no impact on the community structure at $\gamma = 2.5$ and $\gamma = 5$ (Figure 1 e and f/marker 1). Marker 1 denotes a community that fits to the District 15 in both resolutions but is also crossed by freeway M3, a multilane road with physical separation from its surrounding that connect downtown of Budapest to cities in East Hungary. On the contrary, a major road separates mobility communities in the Southeast of the city (Figure 1/marker 2). The bright green community, denoted with marker 2, does not fit to administrative boundaries but is perfectly limited by the freeway M5 and by the river Danube. Finally, physical and administrative boundaries might align, as we see in the case of District 21 in Budapest (Figure 1 b, c, e, f/marker 3). This district that is depicted by marker 3 is bounded by the river Danube and its fork and thus, it constitutes a community in the mobility network not only at the two displayed values of the resolution parameter but in further settings too (see Supplementary Section S4 for details). Note that the features of a physical barrier can affect its community-forming power as Figure 1 show lower order roads (displayed by dotted lines) seem to have no impact on communities at lower resolution, but higher order roads do (e.g., Figure 1/marker 2 or 3). As expected, the communities detected with higher resolution parameter are smaller. However, this trend is more true in the downtown, while communities with the markers 1-3 remained almost the same.

Regarding the heterogeneity of the barrier impact, it is unclear how long-distance versus local mobility is affected. To provide a better understanding, we first compare the role of higher- versus lower rankings of physical or administrative barriers. Next, we test whether those who commute or travel from further away are less likely to be affected by barriers. We finally complement the analysis by checking how visited locations differentiate the barrier impact.

We propose two indicators to evaluate how administrative and physical boundaries fragment mobility networks by quantifying the fit of mobility clusters detected by the Louvain method at various levels of the resolution parameter. The Symmetric Area Difference (SAD) index, SAD_γ captures the lack of overlap between the polygons defined by mobility clusters and the polygons delineated by characteristic urban barriers for every resolution γ (Figure 2a). Formally,

$$SAD_\gamma = \frac{1}{n} \sum_{p,q} (A_{p_\gamma} \cup A_q) \setminus (A_{p_\gamma} \cap A_q), \quad (2)$$

where A_p and A_q are the area sizes of the overlapping mobility cluster polygons p and urban area polygons q and n is the number of iterations of the Louvain community detection at resolution γ . Lower values of this index mean a better fit of the detected mobility clusters to urban boundaries.

Next, we define the Barrier Crossing Ratio (BCR) index, BCR_γ measures the relationship between those mobility events that cross barriers and those that cross barriers and detected mobility clusters as well (Figure 2b). We calculate

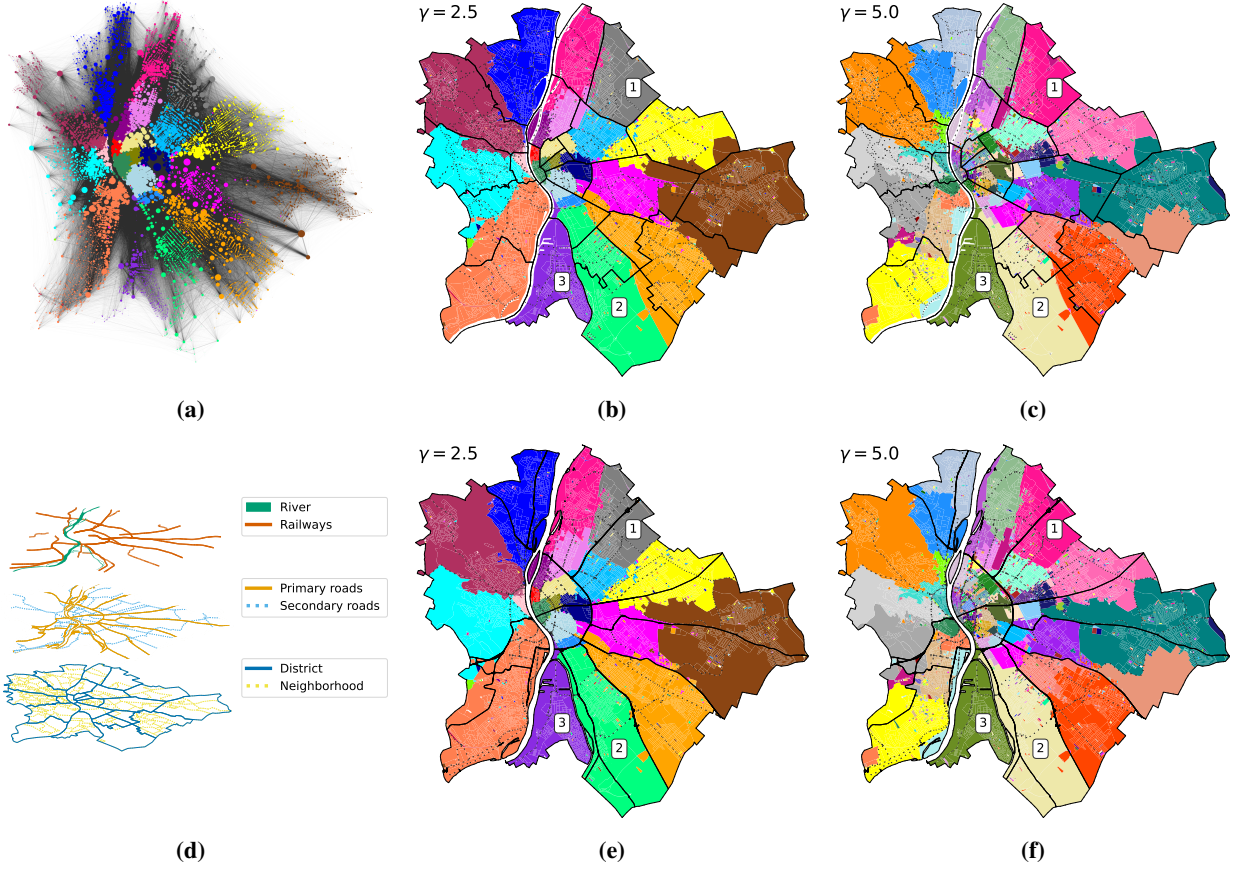


Figure 1: Illustration of the mobility network and the research problem. The observed mobility network (a), where the node sizes are proportional to the degree of a node and the colors represent the detected communities at resolution 2.5. The “layers” of the barriers (d) analyzed in the study include relatively rare natural (river) and built (railways) barriers and relatively frequent ones that also have hierarchical orders like roads (primary and secondary roads) or boundaries administrative urban units (districts and neighborhoods). Mobility clusters detected with resolution parameter $\gamma = 2.5$ (b, e) and $\gamma = 5$ (c, f) compared to administrative boundaries (b, c) and to roads (e, f).

the fraction of barrier and cluster crosses among all barrier crossings, and take the inverse of this ratio. This indicator is formalized by

$$BCR_\gamma = \frac{1}{n} \frac{\sum_m CB(M_k^i, U)}{\sum_m (CB(M_k^i, U) \times CC(M_k^i, C_\gamma))}, \quad (3)$$

where m is the total number of mobility edges, CB is a binary function that evaluates to 1 if M_k^i , the k^{th} mobility edge from block i , crosses an urban barrier U and 0 otherwise, while the function CC takes the value of 1 if M_k^i crosses mobility clusters and n is the number of Louvain iterations at resolution γ . Since barrier crossings are constant, a decreasing value of the indicator along increasing γ signals that border crossings align with mobility cluster crossings.

Both measures are calculated for $n = 10$ iterations of the community partitioning for all decimal values of $\gamma \in [1, 10]$. Further details about the indices can be found in the Materials and Methods.

Assessing the community fit to urban barriers with Symmetric Area Difference

To present a benchmark for urban barrier assessment, we first investigate their impact on urban mobility by testing a widely-used gravity model, in which the volume of mobility flow between block i and j is estimated by their Euclidean distance, the sum of their incoming and outgoing flows and the number of barriers between them (for more details see Materials and Methods). We find that river Danube has the strongest impact on mobility and railways

have the weakest (Figure 3a). Further, there are barriers that have hierarchical relations within the category, such as administrative boundaries can be defined at the higher rank of districts or at the lower rank of neighborhoods; while roads can be primary or secondary. In the gravity model, we find no clear pattern whether higher or lower rank barriers in these hierarchies have a stronger impact on mobility. While boundaries of districts have a bigger impact than neighborhood borders, the coefficient of secondary roads is stronger than that of primary roads. Yet, the gravity model measures an average impact of barriers disregarding the locations of mobility links. On the contrary, a network of mobility links is denser in the center of cities. By finding smaller scales of mobility clusters in high-density areas, our approach provides a better way to understand hierarchies of barriers because we can fit mobility clusters to lower-rank administrative barriers too.

Indeed, assessing the fit of mobility clusters to urban barriers with the SAD_γ indicator, we find that barrier hierarchies have a more intuitive imprint on mobility than in the gravity model. As γ increases in its low ranges, SAD_γ decreases for both district and neighborhood boundaries (Figure 3b). However, the fit to district boundaries reaches a maximum at higher values of γ , while to the fit to neighborhoods further improves as the algorithm finds smaller and smaller groups of blocks that tend to represent mobility clusters at the scale of neighborhoods. A similar trend is found in terms of road hierarchy as γ grows, community detection fits to primary and secondary roads, but at high values of γ the technique provides an improving fit to the secondary roads only (Figure 3c).

Comparing the period that precedes the COVID-19 pandemic with the period that contains the second and third waves of the virus diffusion, the increasing coefficients of the gravity model inform us about an increasing impact of all types of urban barriers on mobility (Figure 3a). However, according to the SAD indicator, the fit of detected communities gets worse for both levels of administrative boundaries and for secondary roads as well. The worsening fit during the pandemic might be due to the drastic drop of mobility links (ca. 33% of the links are present). However, the growth of SAD values at given γ values are not drastic. In the case of primary roads, one can observe that the fit does not differ between the two periods at $\gamma > 3.5$ that also includes the best fit we find. Thus, the community detection method provides stable results for primary roads across very different periods in terms of mobility habits.

In the case of primary roads, we find a characteristic level of the resolution parameter ($\gamma \approx 4$) that provides the best fit of communities. Up to this resolution parameter, the fit measured by SAD_γ improves but the fit gets worse at higher values of γ . This optimal fit arises due to local mobility clusters that emerge after we decrease the dominance of mobility links between large transportation hubs by increasing γ (see Equation 1).

A potential explanation of the worsening fit in Figure 3c can be that local mobility events cross primary roads. However, it may also be that the role of a certain barrier weakens because another one replaces it. Indeed, Figure 4 illustrates an example where such a replacement happens using the case of marker 1 in Figure 1e. The fit to the administrative boundary of District 15 is weak at $\gamma = 1$ when the mobility cluster covers a relatively large area (Figure

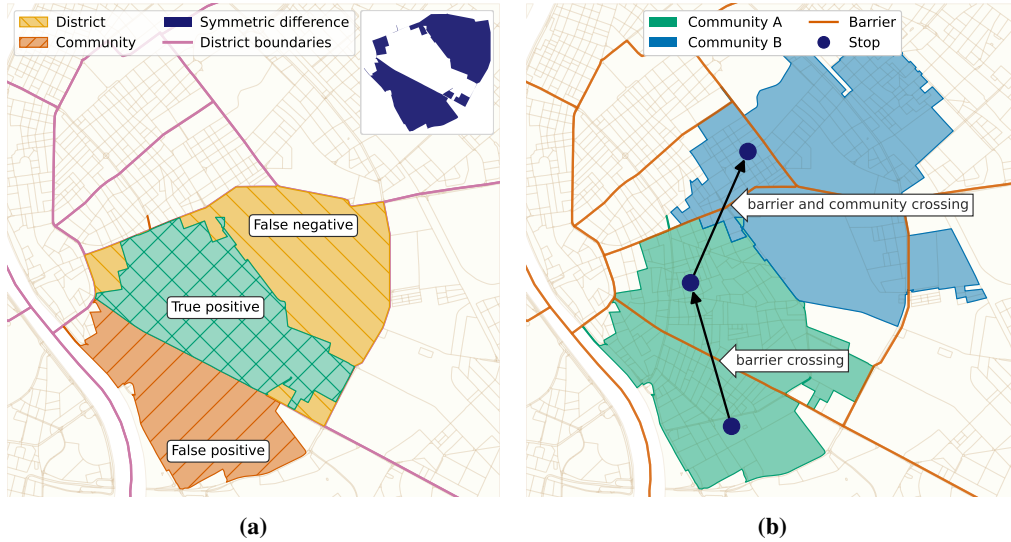


Figure 2: Illustration of indicators used to assess the fit of detected mobility communities to urban barriers. The Symmetric Area Difference (SAD) (a) measures the sum of the areas that are not overlapping between detected mobility clusters and the areas delineated by the given barrier. The Barrier Crossing Ratio (BCR) quantifies the fraction of those trips that cross barriers and mobility clusters as well among all barrier crossing movements (b).

4a) but becomes reasonably good in the range of $\gamma \in (3; 6)$. Further increasing the parameter, we find that the smaller scale mobility cluster fits to the administrative border in the south but is limited in the north by the major road that cuts the district into two. The local mobility cluster is bounded by a combination of barriers that worsens the fit of a single category and suggests that it is not just single barriers that impact mobility but they can influence mixing in more complex configurations.

The fit of mobility clusters to the railways and the river can be found in Supplementary Section S5. The fit of railways during COVID restrictions quantified by SAD_γ is of the same level with districts or primary roads but fits worse at large γ in the pre-COVID period. The SAD_γ values of the fit to the river decrease as γ increases.

Repeating the analysis on a distinct data set from Nagoya, Japan [38], we find that the SAD_γ indicator describes the role of administrative barriers in urban mobility similarly (see Supplementary Section S10). By increasing the resolution parameter γ , the fit of mobility clusters to administrative barriers improves, while it is significantly better for lower-rank boundaries for all γ .

Barrier Crossing Ratio by home locations and amenity mix at destinations

Urban barriers might have a divergent impact on neighborhoods as individuals daily mobility depends largely on the locations of work, schools, and services that are unevenly distributed in and around cities. Thus, in the next step of the analysis, we assess the role of barriers in mobility by decomposing the set of individuals by areas of residence and by visited amenities. To do that, we leverage the home locations of individuals identified in [12] by the device location during the 8pm-8am daily periods and the amenity portfolio of stop locations measured in the same paper. As many people commute from the agglomeration to the capital [39], not only the inhabitants of Budapest are taken into consideration, but people living in the larger agglomeration as well. We use the urban area definition of Hungarian Central Statistical Office (HCSO) to distinguish seven district groups within the city of Budapest and sort municipalities into six sectors of the Budapest agglomeration to group home locations [40] (visualized in Figure 5a). Then, we use the mobility network across Budapest blocks described in Figure 1 to quantify the tendency that individual mobility events cross urban barriers and detected mobility clusters, using the Barrier Crossing Ratio (Eq. 3) that can be decomposed by origins and destinations of mobility events.

We find a striking difference between the BCR indicator of those dwellers who live in the city and those who live in its agglomeration (Figure 5). In every barrier category, agglomeration sectors have higher BCR values than sectors of the city, indicating that commuters from the agglomeration cross relatively more urban barriers without crossing boundaries of mobility clusters than residents of city sectors do. Except the river, the value of BCR is above 1

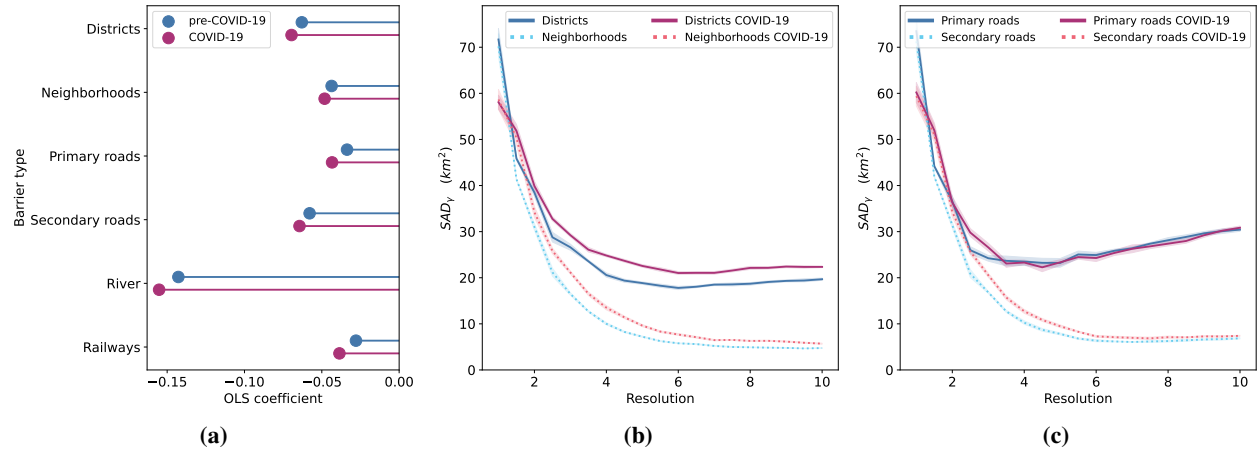


Figure 3: Barrier effect on urban mobility in the gravity and the mobility network approach, preceding and during COVID-19 restrictions. The coefficients of ordinary least squares (OLS) regression measure barrier impact on flows between two locations (a). In (b, c), the lines and shaded area represent the mean and the 95 % confidence interval of the Symmetric Area Difference (SAD) indicator as a measure of barrier fit of mobility clusters detected in ten iterations of the Louvain method for every γ . The improving fit to administrative boundaries along the increasing resolution parameter (b) signals that lower-rank boundaries tend to align with local mobility clusters. This is the case for secondary roads as well but the optimal fit to primary roads at $\gamma \approx 4$ suggests that emerging local mobility clusters are less bounded by primary roads (c).

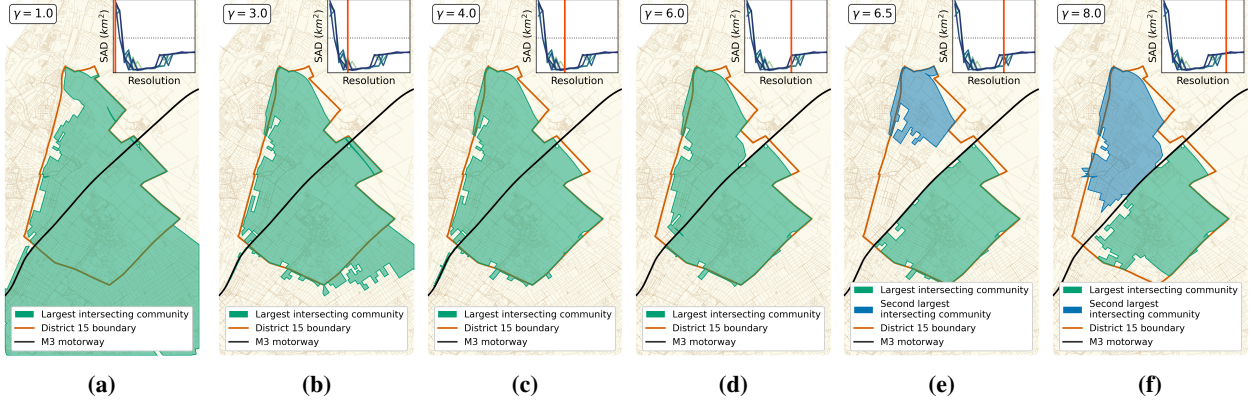


Figure 4: The process of community fitting to District 15 and inset figures show the Symmetric Area Difference (SAD) in respect of the resolution. Note that the largest intersecting community at $\gamma = 1.0$ (a) is about twice as big as the district. As the resolution increases the community matches the district boundary (b, c), which loses the community forming power at about $\gamma = 6.0$, as the M3 motorway gradually cuts in half the community (d–f).

for agglomeration sectors for the lowest γ values in the case of all other barriers. This indicates that the number of total barrier crossings is higher than those crossings that are across barriers and mobility clusters at the same time. Increasing γ provides a better fit of mobility clusters to barriers, in which the differences between urban and agglomeration sectors are stable as γ grows.

Thus, the detected mobility clusters fits urban barriers better for those who live close to these actual barriers than for those who live farther away. Naturally, people living in the agglomeration have different mobility patterns than urban dweller their vast majority use cars when commuting to the city but also optimize home and work location so that they usually commute to the closest part of the capital. For example, people living in the Northwestern sector visit mostly North Buda and only a small portion of their visits are located in the inner Eastern Pest (see the sectors in Figure 5a and Supplementary Section S7 for details). However, North Buda and South Buda behave like agglomeration sectors at low levels of γ in the case of Primary roads and Railways but perform a relatively good fit to barriers at high γ .

The Danube as barrier has the strongest impact on mobility. Interestingly, the ratio of barrier crossings and mobility cluster crossings is nearly constant across values of γ for most sectors, meaning that local mobility flows hardly cross the river. In other words, crossing the river almost automatically means crossing mobility clusters too. This is especially true for residents of the agglomeration: 90% of their crossings over the river leads to other mobility clusters. The Supplementary Section S6 contains further analyses in respect of the residence-based mobility networks, including another evaluation of the BCR where separate networks were generated for the urban areas. This approach takes into consideration that commuting distance impacts mobility patterns that can be captured by different mobility networks. Yet, these results also confirm that urban barriers in Budapest have a stronger impact on urban dwellers than on commuters.

Interestingly, we see a different pattern for Nagoya (Supplementary Section S10) where we could evaluate the fit of mobility clusters to municipality boundaries and primary roads using the BCR_γ index. Residents of the city have higher BCR_γ values suggesting that they cross urban barriers that are also barriers of mobility clusters more often than residents of agglomeration towns. Thus, local contexts have an important role in distinguishing the impact of urban barriers on dweller groups that further research should focus on.

Next, we calculate the Barrier Crossing Ratio (BCR) indicator for individuals, instead of areas. Since the mobility network is aggregated from individual trips, one can compare the barrier and mobility cluster crossings at the individual level in the same ways as it is introduced in Section Barrier Crossing Ratio. The individual Barrier Crossing Ratio (BCR) captures the average BCR of individual citizen c in the n^{th} run of the community detection with resolution γ . The indicator takes a lower value for those individual citizens who cross barriers by visiting mobility clusters and takes a larger value for those who cross barriers without leaving the mobility cluster.

This measure enables us to investigate how the role of barriers depends on home locations and also on visited amenities in a multivariate analysis. We regress BCR with an Ordinary Least Squares (OLS) linear regression, using the formula:

$$\log BCR_{\gamma,n}^c = \alpha + \beta_1 \log D_c + \beta_2 \log AC_j + \epsilon, \quad (4)$$

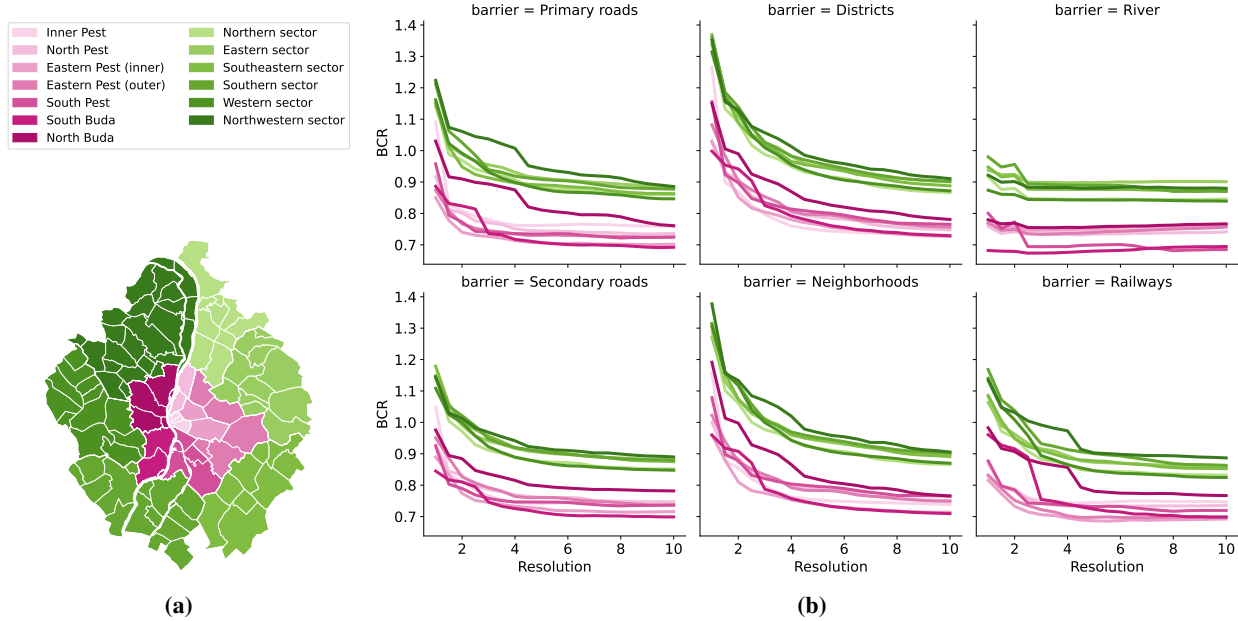


Figure 5: Barrier effect based on the users' home location groups. The HCSO defines seven district groups in Budapest and six sectors of the agglomeration (a). From the Budapest mobility of the inhabitants of these areas, thirteen networks were built and evaluated for all barrier type with the BCR_γ index and increasing the γ parameter (b).

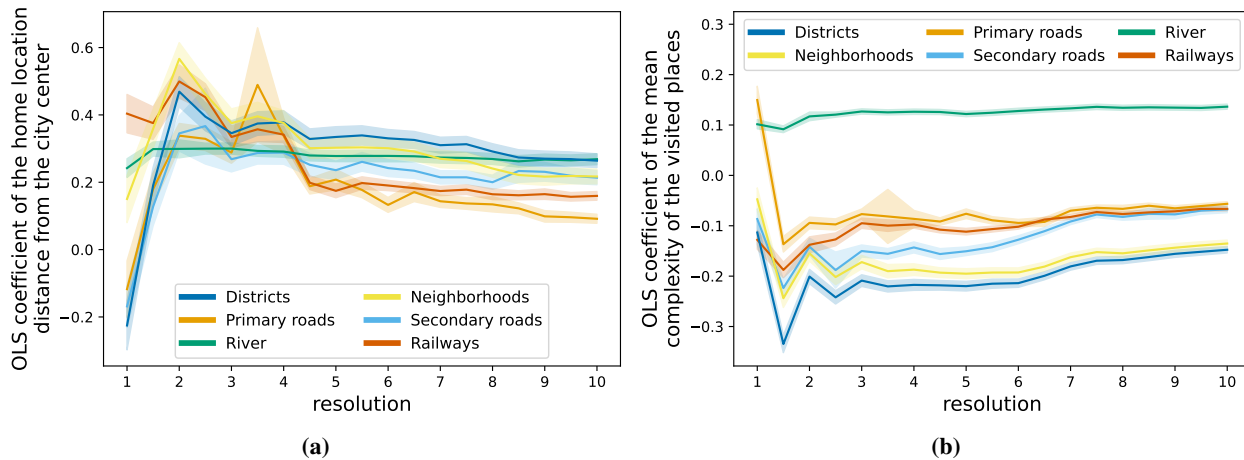


Figure 6: Urban barrier impact on individuals by distance from the center and by visited amenities. We depict the relationship between Barrier Crossing Ratio and the distance between the inhabitants home location and the city center (a) and the mean location complexity of the visited places (b). Solid lines represent estimation coefficients and the shaded area denotes standard errors.

where D_c is the geographical distance of the home location of citizen c from the city center and AC_j is the complexity of amenity portfolio of the visited j location as proposed by [12] and ϵ is the error term. Amenity complexity is high in those locations that host diverse services that are difficult to find elsewhere in the city. Locations with complex amenity portfolios have been found to promote social mixing because they serve a diverse demand and can attract visitors from the whole city [12].

The findings reveal significant relationship between the distance, amenity complexity and Barrier Crossing Ratio that also seems to be stable $\gamma > 1.5$ for all types of barriers (Figure 6). As expected, D_c correlates positively with BCR (Figure 6a) confirming our previous finding that those who live farther away from the center are more likely to cross barriers without crossing mobility clusters because the fit of the detected cluster is worse for them. However, we find

a negative correlation between AC_j and BCR for most types of barriers. This result suggests that visiting complex amenities that are in other mobility clusters, individuals usually cross urban barriers too. The river seems to be an exception here as well, but as discussed above, there are rarely any mobility clusters that extend across the river; thus, BCR calculation in this case could only consider visits to two islands that are sharing mobility clusters with districts on the Pest side. The stable coefficients of D_c and AC_j over γ signals that relationship with BCR is not an artifact of community sizes; instead, these correlations capture a general impact of barriers on mobility, considering complex structures of mobility networks. The OLS tables are in the supplementary section S9.

Discussion

Urban barriers are obstacles of social interactions and even the built urban infrastructure, which is aimed to facilitate access, can hinder mobility. Here we apply a network science framework that provides a new understanding of this phenomenon and enables us to investigate how urban barriers delineate clusters of mobility considering complex network structures. Our results demonstrate that besides natural and administrative boundaries, major roads within cities can separate individuals. We explore that mobility clusters can be impacted by combinations of barrier types. We also discover that barriers has a smaller impact on mobility to complex amenity locations because these places attract visits from many neighborhoods. In the case of Budapest, urban barriers better align with mobility clusters of urban dwellers and less so for residents who live in the larger metropolitan area and commute to the city. However, we find a different pattern in the case of Nagoya, where barriers have a bigger impact on commuters. Thus, the question why the barrier impact come to be and how it differs across groups of citizens is open. Further research should therefore investigate the role of local economic environment, the transportation system, commuting trends, social segregation, and urban geography in general to better understand what makes urban barriers impact mobility.

The strong impact of barriers has wide-ranging implications for the ongoing discussion of social mixing in cities [41, 12, 42, 9, 10]. Similarly to the role of mobility restrictions that have been documented to increase urban segregation [11, 43], urban barriers can hinder the mixing of individuals from various socio-economic strata, even if they live only on the opposite sides of roads or railroads [26]. Such separation can foster segregation in social networks and can lead to growing inequalities [27]. Therefore, the impact of barriers on mobility should be considered in recent proximity-based urban developments - that are often referred to as the 15-minute city concept - that aim to foster short distance active mobility and inclusion in cities. We need a better understanding how improving access to amenities [44, 15], which are reachable with active mobility, can overcome urban barriers like major roads that still channel the flows of larger distance car traffic.

Our study is not without limitations. As the mobile positioning data used in this study does not have information about the means of transport, it is not possible to differentiate between pedestrians, bikers, public transport passengers or car drivers. A possible future direction is to use additional data sources, e.g. from bike sharing services, to analyze the barrier effect on bikers. Such advances could help improve the bicycle lane infrastructure and detect possibly dangerous spots that behave string barriers for bikers. Using further data from public transport usage could help us understand how public transport contributes to the emergence of mobility clusters. Future work should investigate the circumstances of community formation in mobility networks across a variety of cities. To highlight the separation power of built infrastructure, we have to compare different trajectories of urban evolution that has led to the dominance of administrative boundaries or, on the contrary, to the dominance of roads in delineating mobility clusters. Finally, we need further research that focuses on mixing of strata across urban barriers and the types of mobility that can decrease experienced segregation given the boundaries in cities.

Materials and Methods

Mobility Data

The mobility data was collected by a data aggregator company from various unspecified smartphone applications. Some applications – e.g., navigation – leaves frequent traces leaving a continuous trajectory, but other applications generated sporadic traces. A record contains a timestamp, a user ID, and a GPS location. The data covers whole Hungary. We limit the analysis to mobility events in Budapest. The observation period is six months from September 2019 and another six months starting from November 2020. The raw pings were processed by applying the Infostop algorithm [32]. It can detect the stationary points of individual movements and cluster pings around locations, where the individual stopped. The algorithm gives each stop a label indicating a place that can reoccur along the trajectory of the user. The process is detailed in a previous work of the authors [12]. This procedure has enabled us to identify home locations by detecting stops between the 8pm-8am hours. In the BCR exercise, we limit the observations to those users who have home locations in Budapest or in municipalities in the Budapest agglomeration.

Barrier Data

In this paper, administrative, natural and infrastructural barriers are also considered, which were obtained from OpenStreetMap (OSM). As for the administrative boundaries, administrative level 9 (districts) and 10 (neighborhoods) is utilized. Budapest has 23 districts and 207 urban neighborhoods. Note that neighborhoods are in between districts and census tracts in the spatial hierarchy. The OpenStreetMap classifies the roads based on their hierarchy. For this study, the motorways, the primary and secondary roads are considered. In the OSM terminology, trunks are between motorways and primary roads, however they are not significant in Budapest. Motorways are merged with the primary roads, since they cannot enclose areas on their own. Illustrated in Figure 1d by solid orange lines. Secondary roads are less important than primary roads in the OSM highways hierarchy and they limit smaller areas than primary roads. The primary roads divide the city into some larger parts, and with the secondary roads into smaller parts. A script was developed to create polygons from the city parts enclosed by the roads, for details see Section S3 in the Supplementary Materials.

Mobility Network and Community Detection

When all the lower order roads are also considered during the polygon creation, the enclosures denote blocks. Then, the places from the mobility data are mapped to the blocks, which will be the nodes of a network. Two blocks are connected by an edge if a user had consecutive places between the given blocks within a day. The places are considered only within a day because of the sporadic nature of the data. It is undesired to connect a user's last position of a day to the first position of the next day. Naturally, a threshold could be introduced as if a user is active in the night, a valid mobility trajectory is broken at midnight. This, however, is a possible direction of future enhancements.

The Louvain community detection [29] is applied to the stop-network with different resolution values, that clusters the blocks into communities. Due to the nondeterministic nature of the community detection algorithm, it was executed ten times for every resolution value. The stability of the community detection across executions was examined using Cramér's V, which can be found in the supplementary section S2. Then, the values of the difference executions were aggregated.

Gravity Model

The gravity model [45] is a widely used method for activity distance and border effect measuring [17]. Originally, the gravity model for mobility flow is formalized a $Mob_{i,j} = k \frac{P_i^\alpha P_j^\beta}{r_{i,j}^\gamma}$, where $Mob_{i,j}$ is the mobility between spatial unit i and j , P_i is the population in unit i , and $r_{i,j}$ is the distance between spatial units i and j , and k , α , β , and γ are constant parameters [17].

The original formula is extended with the number of crossed barriers, one by one to measure the effect of the given barrier type. When counting the crossed barriers between two blocks, the beeline is considered between the centroid of the block as the mobility data does not contain any information about the way of transport. So, every barrier is counted – by type – which the straight crosses. As for the distance ($r_{i,j}$), the haversine (great-circle) distance is used between the two block centroids. The model (5) was evaluated using the Ordinary Least Squares (OLS) regression. The barrier variables have been inserted separately to the regression model due to their high correlation.

$$\begin{aligned} \log Mob_{i,j} = & \alpha \log P_i + \beta \log P_j + \gamma \log D_{i,j} + \delta \log road^p \\ & \delta \log road^s \\ & \delta \log river \\ & \delta \log railways \\ & \delta \log district \\ & \delta \log neighborhood \end{aligned} \quad (5)$$

Symmetric Area Difference

It is a known feature of the Louvain community detection algorithm that by increasing the resolution parameter, the size of the communities decreases. The hypothesis was that the community sizes did not only decrease arbitrarily but converge to the barriers. To confirm this assumption, the similarity of the communities and the enclosures had to be measured. The area of the blocks clustered as a community, but outside the target polygon (e.g., district or enclosure) and the area of the target polygon that is not covered by the community is summarized as a measure. In other words,

the area of the false positive and the false negative blocks, which is the symmetric difference of the two polygons (Figure 2a).

The changes in the community areas are evaluated in respect of the administrative and infrastructural barriers during the change of the resolution parameter with the symmetric area difference between the clustered blocks (i.e., community) and the administrative districts.

Barrier Crossing Ratio

The barrier crossings are counted for every barrier type, also used in the gravity model. It is also counted if a barrier crossing The count of the barrier crossings that also represent a community crossing (Figure 2b) also determined. The quotient of these two values is called crossing ratio, calculated as $\frac{BC^{obs}}{CC^{obs}}$, where BC is the barrier crossing and CC is the barrier crossing that is also a community crossing. As the resolution parameter of the Louvain community detection algorithm is increased, the communities become smaller, which means that the trips crosses communities with higher probability. Barrier crossing does not depend on the resolution, it is a constant, while the CC is increasing as the communities become smaller. Thus, the quotient is decreasing, which can be seen in Figure S10a and S10b of the Supplementary Materials.

Acknowledgement

The authors acknowledge the help of Endre Borza with the initial data processing and the stop detection as a part of [12]. Useful comments have been received at the NetMob23 Conference in Madrid, the NetSci23 Conference in Vienna.

Data and Code Availability

The barrier data is obtained from OpenStreetMap; these data are copyrighted by the OpenStreetMap contributors and licensed under the Open Data Commons Open Database License (ODbL).

The observed mobility networks will be available via Zenodo under ODbL, and the code, that will be published in GitHub, the results are reproducible. However, the raw mobile positioning data is not publicly available.

References

- [1] Jane Jacobs. *The death and life of great American cities*. Vintage, 2016.
- [2] Raj Chetty, Nathaniel Hendren, and Lawrence F Katz. “The effects of exposure to better neighborhoods on children: New evidence from the moving to opportunity experiment”. In: *American Economic Review* 106.4 (2016), pp. 855–902.
- [3] Ana V Diez Roux. “Investigating neighborhood and area effects on health”. In: *American journal of public health* 91.11 (2001), pp. 1783–1789.
- [4] Robert J Sampson and Stephen W Raudenbush. “Systematic social observation of public spaces: A new look at disorder in urban neighborhoods”. In: *American journal of sociology* 105.3 (1999), pp. 603–651.
- [5] Huiping Li, Harrison Campbell, and Steven Fernandez. “Residential segregation, spatial mismatch and economic growth across US metropolitan areas”. In: *Urban Studies* 50.13 (2013), pp. 2642–2660.
- [6] Marta C. González, César A. Hidalgo, and Albert-László Barabási. “Understanding individual human mobility patterns”. In: *Nature* 453 (7196 2008), pp. 779–782.
- [7] Laura Alessandretti, Ulf Aslak, and Sune Lehmann. “The scales of human mobility”. In: *Nature* 587 (2020), pp. 402–407.
- [8] Markus Schläpfer et al. “The universal visitation law of human mobility”. In: *Nature* 593.7860 (2021), pp. 522–527.
- [9] Susan Athey et al. “Estimating experienced racial segregation in US cities using large-scale GPS data”. In: *Proceedings of the National Academy of Sciences* 118.46 (2021), e2026160118.
- [10] Zhuangyuan Fan et al. “Diversity beyond density: Experienced social mixing of urban streets”. In: *PNAS nexus* 2.4 (2023), pgad077.
- [11] Takahiro Yabe et al. “Behavioral changes during the COVID-19 pandemic decreased income diversity of urban encounters”. In: *Nature Communications* 14.1 (2023), p. 2310.

- [12] Sándor Juhász et al. “Amenity complexity and urban locations of socio-economic mixing”. In: *EPJ Data Science* 12.1 (2023), p. 34.
- [13] Xiaowen Dong et al. “Segregated interactions in urban and online space”. In: *EPJ Data Science* 9 (2020), pp. 1–20.
- [14] Qi Wang, Mario L. Small Nolan Edward Phillips, and Robert J. Sampson. “Urban mobility and neighborhood isolation in America’s 50 largest cities”. In: *Proceedings of the National Academy of Sciences* 115 (30 2018), pp. 7735–7740.
- [15] Timur Abbiasov et al. *The 15-minute city quantified using mobility data*. Tech. rep. National Bureau of Economic Research, 2022.
- [16] Hamed Nilforoshan et al. “Human mobility networks reveal increased segregation in large cities”. In: *Nature* 624.7992 (2023), pp. 586–592.
- [17] Meihan Jin et al. “Identifying borders of activity spaces and quantifying border effects on intra-urban travel through spatial interaction network”. In: *Computers, Environment and Urban Systems* 87 (2021), p. 101625.
- [18] Mylena Cristine Rodrigues de Jesus and Antônio Néelson Rodrigues da Silva. “Barrier Effect in a Medium-Sized Brazilian City: An Exploratory Analysis Using Decision Trees and Random Forests”. In: *Sustainability* 14.10 (2022), p. 6309.
- [19] Alisa W Coffin. “From roadkill to road ecology: a review of the ecological effects of roads”. In: *Journal of transport Geography* 15.5 (2007), pp. 396–406.
- [20] Ronald Villalobos-Hoffman, Jack E Ewing, and Michael S Mooring. “Do Wildlife Crossings Mitigate the Roadkill Mortality of Tropical Mammals? A Case Study from Costa Rica”. In: *Diversity* 14.8 (2022), p. 665.
- [21] Jan Olof Helldin and Silviu O Petrovan. “Effectiveness of small road tunnels and fences in reducing amphibian roadkill and barrier effects at retrofitted roads in Sweden”. In: *PeerJ* 7 (2019), e7518.
- [22] Paulo Anciaes and Peter Jones. “A comprehensive approach for the appraisal of the barrier effect of roads on pedestrians”. In: *Transportation research part A: policy and practice* 134 (2020), pp. 227–250.
- [23] Savvas Emmanouilidis et al. “Settlements along Main Road Axes: Blessing or Curse? Evaluating the Barrier Effect in a Small Greek Settlement”. In: *Land* 11.12 (2022), p. 2243.
- [24] Job van Eldijk et al. “Missing links—Quantifying barrier effects of transport infrastructure on local accessibility”. In: *Transportation Research Part D: Transport and Environment* 85 (2020), p. 102410.
- [25] Yunmi Park and George O Rogers. “Neighborhood planning theory, guidelines, and research: Can area, population, and boundary guide conceptual framing?” In: *Journal of Planning Literature* 30.1 (2015), pp. 18–36.
- [26] Elizabeth Oltmans Ananat. “The wrong side (s) of the tracks: The causal effects of racial segregation on urban poverty and inequality”. In: *American Economic Journal: Applied Economics* 3.2 (2011), pp. 34–66.
- [27] Gergő Tóth et al. “Inequality is rising where social network segregation interacts with urban topology”. In: *Nature Communications* 12 (1143 2021), pp. 1–9.
- [28] Luca Maria Aiello et al. “Urban highways are barriers to social ties”. In: *arXiv preprint arXiv:2404.11596* (2024).
- [29] Vincent D Blondel et al. “Fast unfolding of communities in large networks”. In: *Journal of statistical mechanics: theory and experiment* 2008.10 (2008), P10008.
- [30] Santo Fortunato and Mark EJ Newman. “20 years of network community detection”. In: *Nature Physics* 18.8 (2022), pp. 848–850.
- [31] Paul Expert et al. “Uncovering space-independent communities in spatial networks”. In: *Proceedings of the National Academy of Sciences* 108.19 (2011), pp. 7663–7668.
- [32] Ulf Aslak and Laura Alessandretti. *Infostop: Scalable stop-location detection in multi-user mobility data*. 2020. arXiv: 2003.14370 [physics.soc-ph].
- [33] Stanislav Sobolevsky et al. “Delineating geographical regions with networks of human interactions in an extensive set of countries”. In: *PloS one* 8.12 (2013), e81707.
- [34] Balázs Lengyel et al. “Geographies of an online social network”. In: *PloS one* 10.9 (2015), e0137248.
- [35] Sebastian Grauwin et al. “Identifying and modeling the structural discontinuities of human interactions”. In: *Scientific reports* 7.1 (2017), p. 46677.
- [36] Arnaud Adam, Jean-Charles Delvenne, and Isabelle Thomas. “Detecting communities with the multi-scale Louvain method: robustness test on the metropolitan area of Brussels”. In: *Journal of Geographical systems* 20.4 (2018), pp. 363–386.
- [37] Neave O’Clery and Stephen Kinsella. “Modular structure in labour networks reveals skill basins”. In: *Research Policy* 51.5 (2022), p. 104486.

- [38] Takahiro Yabe et al. “YJMob100K: City-scale and longitudinal dataset of anonymized human mobility trajectories”. In: *Scientific Data* 11.1 (2024), p. 397.
- [39] Gergő Pintér and Imre Felde. “Commuting Analysis of the Budapest Metropolitan Area Using Mobile Network Data”. In: *ISPRS International Journal of Geo-Information* 11.9 (2022), p. 466.
- [40] Központi Statisztikai Hivatal. *Budapest – Gazdaság és társadalom*. ISBN: 978-963-235-541-2. Keleti Károly utca 5-7., 1024 Budapest, Hungary: Központi Statisztikai Hivatal, 2018. ISBN: 978-963-235-541-2.
- [41] Esteban Moro et al. “Mobility patterns are associated with experienced income segregation in large US cities”. In: *Nature Communications* 12 (1 2021), pp. 1–10.
- [42] Eszter Bokányi et al. “Universal patterns of long-distance commuting and social assortativity in cities”. In: *Scientific reports* 11.1 (2021), p. 20829.
- [43] Ludovico Napoli et al. “Socioeconomic reorganization of communication and mobility networks in response to external shocks”. In: *Proceedings of the National Academy of Sciences* 120.50 (2023), e2305285120.
- [44] Yanyan Xu et al. “Deconstructing laws of accessibility and facility distribution in cities”. In: *Science advances* 6.37 (2020), eabb4112.
- [45] Gautier Krings et al. “Urban gravity: a model for inter-city telecommunication flows”. In: *Journal of Statistical Mechanics: Theory and Experiment* 2009.07 (2009), p. L07003.

Supplementary Materials

S1 COVID-19 data set

Six months of mobility data is used before the COVID-19 pandemic (between September 2019 and February 2020) to analyze the barrier effect in urban mobility. As a part of the epidemic prevention strategy, restrictions have been issued, which limited to the mobility.

To compare the barrier effect during the pandemic, another 6-month interval was selected from the available mobile positioning data. In Hungary, the second and third waves took place between the autumn of 2020 and the spring of 2021.

The strictest protocols were issued between 11 November 2020 and the late May 2021, including curfew in nighttime. To match the pandemic data set as close as possible to the pre-pandemic data set, the six months between November 2020 and April 2021 have been selected. Figure S1 shows the selected interval in comparison to the weekly number of deaths during the pandemic.

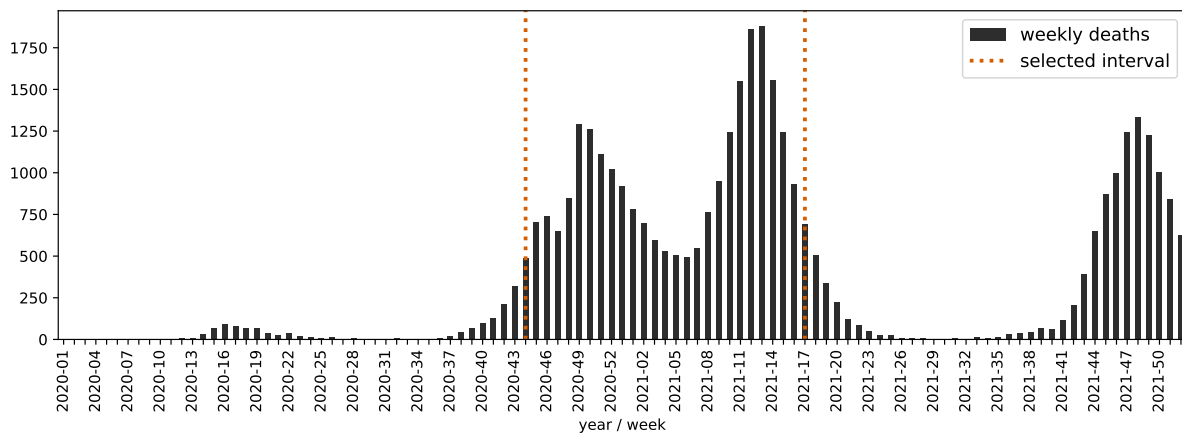


Figure S1: COVID-19 mortality in Hungary between January 2020 and December 2021. The selected interval is considered the second and third wave in Hungary. Data is from European Centre for Disease Prevention and Control [1].

S2 Stability of the community detection

To test the stability of the community detection, the Cramér's V was applied to the communities by resolution. Figure S2a shows the kernel density plots of the Cramér's V values by resolution, with the medians using white dotted lines. At low resolution the median V value is high, but strongly distributed. The median decreases until $\gamma = 6$, then it starts converging to 0.78, while the distribution gets narrower. Furthermore, the trend of the medians is analogous to the Symmetric Area Difference (SAD). Figure S2b show the correlations (Pearson's R) between the medians and the SAD by barrier type. There are strong positive correlations between the barrier types, except the river where the correlation is strong, but negative as the river behaves differently (Figure S5b in contrast to Figure 3).

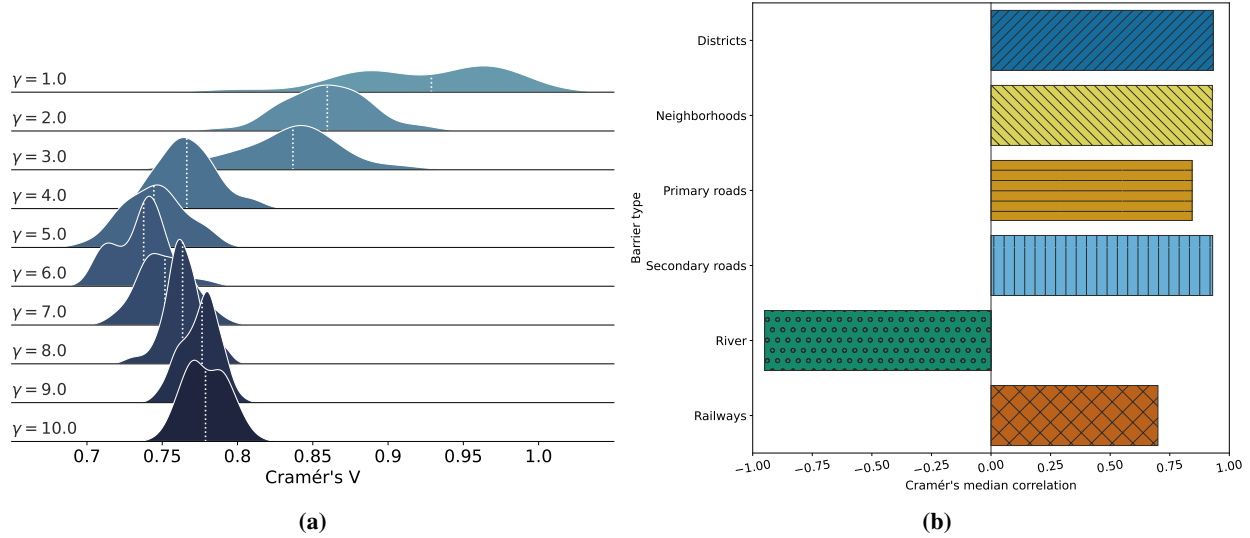


Figure S2: Cramér's V in contrast to the resolution, showing median values with white dotted lines (a), and the correlation (Pearson's R) between the V median and the Symmetric Area Difference (b).

S3 Enclosures

A Python script was developed to obtain enclosed areas from OpenStreetMap (OSM) with different type of roads and other potential barriers, based on [2]. To select the roads that were considered as barriers, the classification system of OSM is used. The script can be parameterized which road types should be included. The road types are taken into consideration in three levels: (i) “primary” including OSM motorway and OSM primary types, (ii) “secondary” which extends the primary with the OSM primary type (Figure S3a), and (iii) every road (Figure S3b). At the third level, the concept is extended to every lower-order streets until the enclosures became blocks.

Note that trunks are omitted from the analysis in this study. Trunks and motorways are not significant within the administrative boundaries of Budapest. There are actually more trunks (27.2 km) than freeway (12.6 km) but freeways continue as primary roads whereas trunk are on the periphery (see Figure S3c) as mostly part of the M0 ring freeway.



Figure S3: Enclosure polygons generated from primary and secondary roads (a) and all roads (b), focusing to Budapest downtown. The ‘motorway’, ‘trunk’ and ‘primary’ road types within Budapest based on OSM data (c).

S4 Symmetric Area Difference Changes

Figure S4 shows the changes in symmetric area differences SAD by the resolution parameter (γ) of the Louvain community detection, for two selected districts. As stated in the main text, District 21 is on an island, which makes its boundaries very stable (Figure S4b). The symmetric area difference is minimal from resolution 2.5, and does not change later. In the case of District 15, it reaches the minimum at about $\gamma = 2.5$ (later during some runs), but it remains more or less stable only until $\gamma = 5.5$ to $\gamma = 6.5$, with some alternation between the community detection runs (Figure S4a). After that point, the community splits up, and the district loses its community-forming power.

Note that the midstream of river Danube is a natural district border between Buda- and Pest-side districts, but that also means that some water surface is part of the administrative area of the districts. As water surfaces are not classified to communities, they were removed from the area of the affected districts.

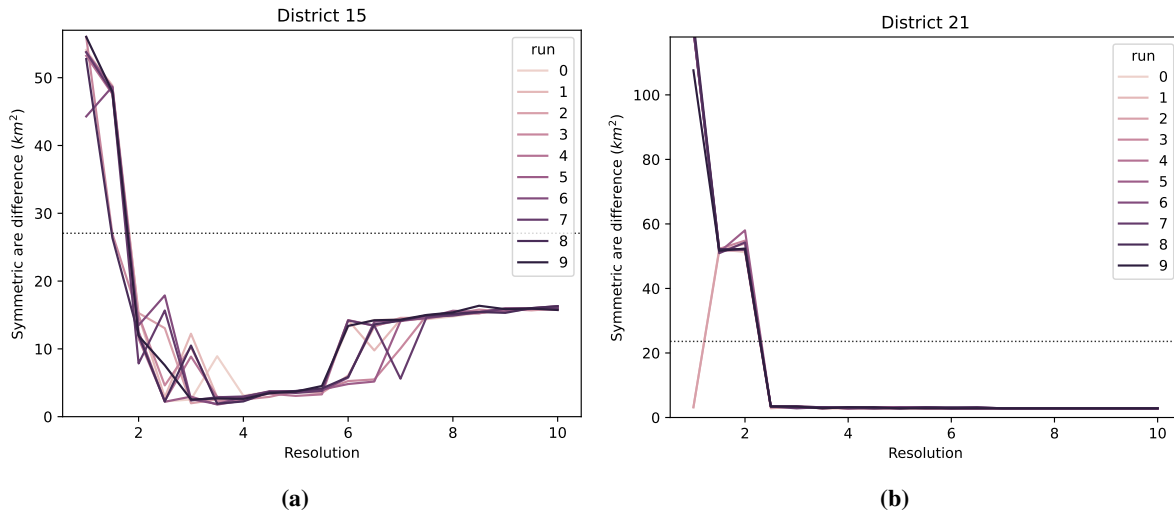


Figure S4: The changes in symmetric area differences by the resolution parameter of the Louvain community detection, in the cases of District 15 (a) and District 21 (b). The dotted line represents the area of the district as a reference.

S5 SAD of Railways and River Barriers

The main text introduces analysis on the community fit to urban barriers with Symmetric Area Difference (SAD) focusing on administrative barriers and the road infrastructure, before and during the COVID-19 pandemic.

As for the railways, the fit is not so strong, and even worse before the pandemic. It has a minimum around $\gamma = 3$. Interestingly, during the pandemic the barriers effect regarding the railways are strengthened, which is the opposite effect as it was in respect of the roads and the administrative boundaries (Figure 3c and 3b of the main text).

Figure S5b show the SAD of the river enclosures. The river Danube divides Budapest to three parts (Figure S5c), excluding Margaret Island and Óbuda Island: Buda, Pest and Csepel (district 21). Although river midstream is the boundary between the Buda and Pest-side districts and definitely a strong natural barrier, the river Danube on its own does not create complete communities, except for District 21 (see Figure S4b). It is because Buda and Pest does not form a community, even at $\gamma = 1$ there are multiple communities both in Buda and Pest (Figure S5d).

Also note that the $\gamma = 1$ communities are roughly approximate the HCSO district group partitioning (Figure S6a), except that Csepel (District 21) is belongs to the South-Pest area and there is a larger green area at the eastern part, where the airport is located, that is in the same community as the Inner-Pest. There is not much residential are near the airport that can explain the size of that community part, but the airport has strong transportation ties to the city center.

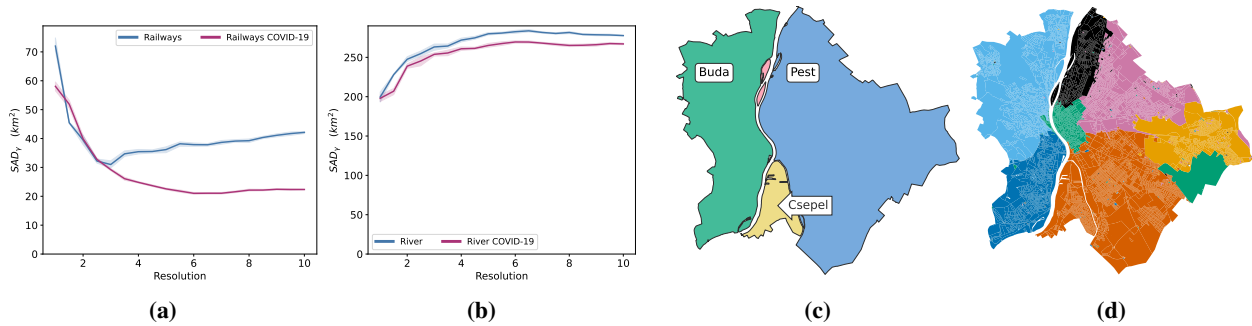


Figure S5: The Symmetric Area Difference (SAD) regarding the railway lines (a) and the river Danube (b). In (a, b), the lines and shaded area represent the mean and the 95 % confidence interval of the SAD indicator as a measure of barrier fit of mobility clusters detected in ten iterations of the Louvain community detection algorithm. The river Danube divides Budapest into three main parts, illustrated in (c). Also, (d) shows a possible community partition at $\gamma = 1$ with the Louvain community detection.

S6 Barrier Crossing Ratio by home locations

Figure S6 shows the same as Figure 5 of the main text, but instead of highlighting the Budapest–agglomeration difference, it uses the different colors for every sector of the agglomeration and district groups of Budapest.

This representation can reveal additional details. In the case of the North Buda regarding the primary roads, the BCR behaves more like the agglomeration at small γ , but more like the rest of Budapest at higher resolution. The reason may be that the Buda-side districts are not divided by primary roads (see Figure S3c), so primary roads cannot form the communities in that area.

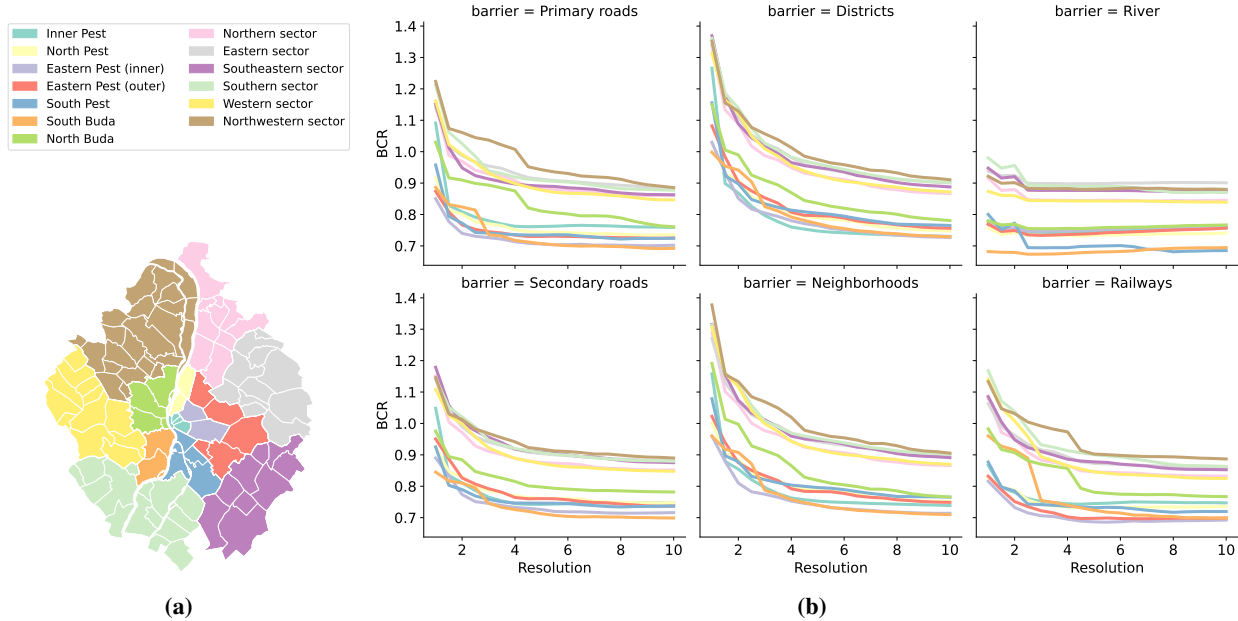


Figure S6: Barrier effect based on the users' home location groups compared to the communities of the original network. Figure a shows the seven district groups in Budapest and six sectors of the agglomeration, defined by HCSO. Figure b shows the changes of the crossing ratio regarding the type of the barrier.

The pre-pandemic network has been divided based on the home locations of the users to thirteen networks. However, the BCR was compared to the original network. Another approach is to determine communities for the new networks and compare the BCR to the those communities. Figure S7 show the BCR compared to the communities of each subnetwork, constructed for the seven district groups of Budapest and six sectors of the agglomeration (defined by HCSO).

The result also shows clear distinction between the Budapest and the agglomeration areas, except the river, where the western sectors of the agglomeration behave much closer to the city than to the eastern sectors. The city center is more complex and attracts more diverse people [3]. Crossing the river Danube seems more probable from the western agglomeration than from the eastern sectors. This assumption is supported by the visitation analysis, presented in Section S7. Furthermore, the order of the sectors remains practically the same for each barrier type. The BCR value of the eastern sectors are higher than the western sectors' for every γ value.

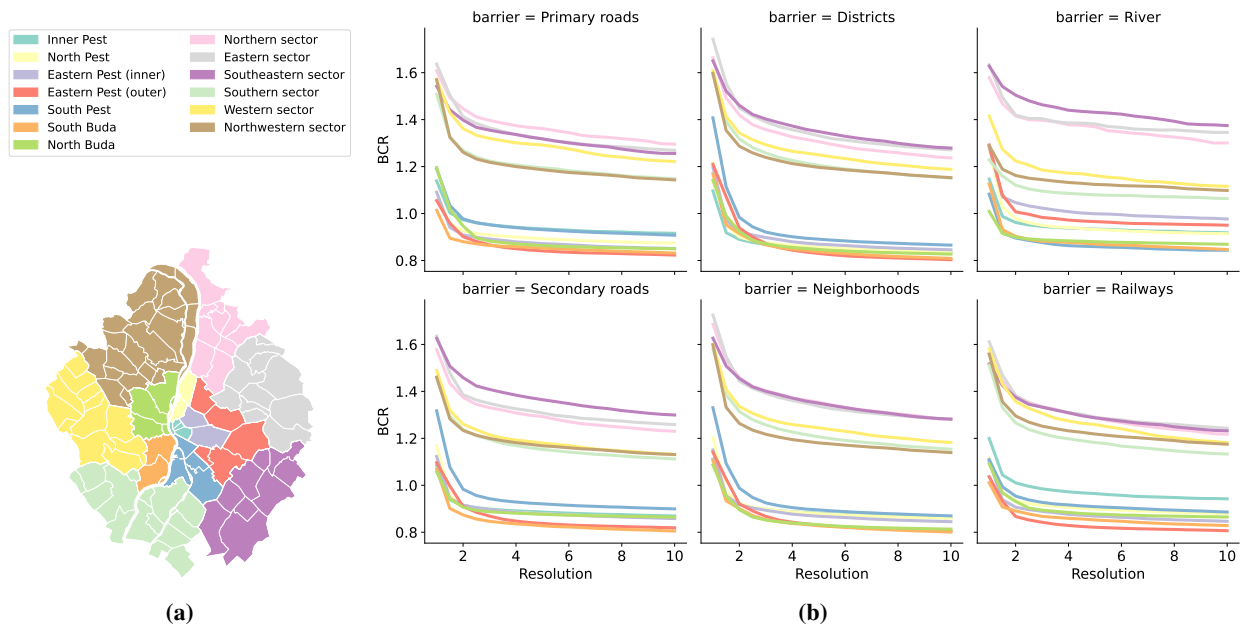


Figure S7: Barrier effect based on the users' home location groups compared to the communities of each subnetwork. Figure **b** shows the changes of the crossing ratio regarding the type of the barrier.

S6.1 Home-location-based Network Details

Figure S8c shows the density of the network. People living in Budapest create more dense networks than the people living in the agglomeration. Figure S8d shows the number of the detected inhabitant to give some context to the network density.

The coefficients of the gravity model are displayed in Figure S8b by barrier categories and home groups. North and South Buda stand closely together in almost every barrier category and differ from the Pest-side district groups. Among the agglomeration sectors there are also some clustering: Northern, Eastern and Southeastern sectors (East of the capital) significantly differ from the Southern, Western and Southwestern sectors.

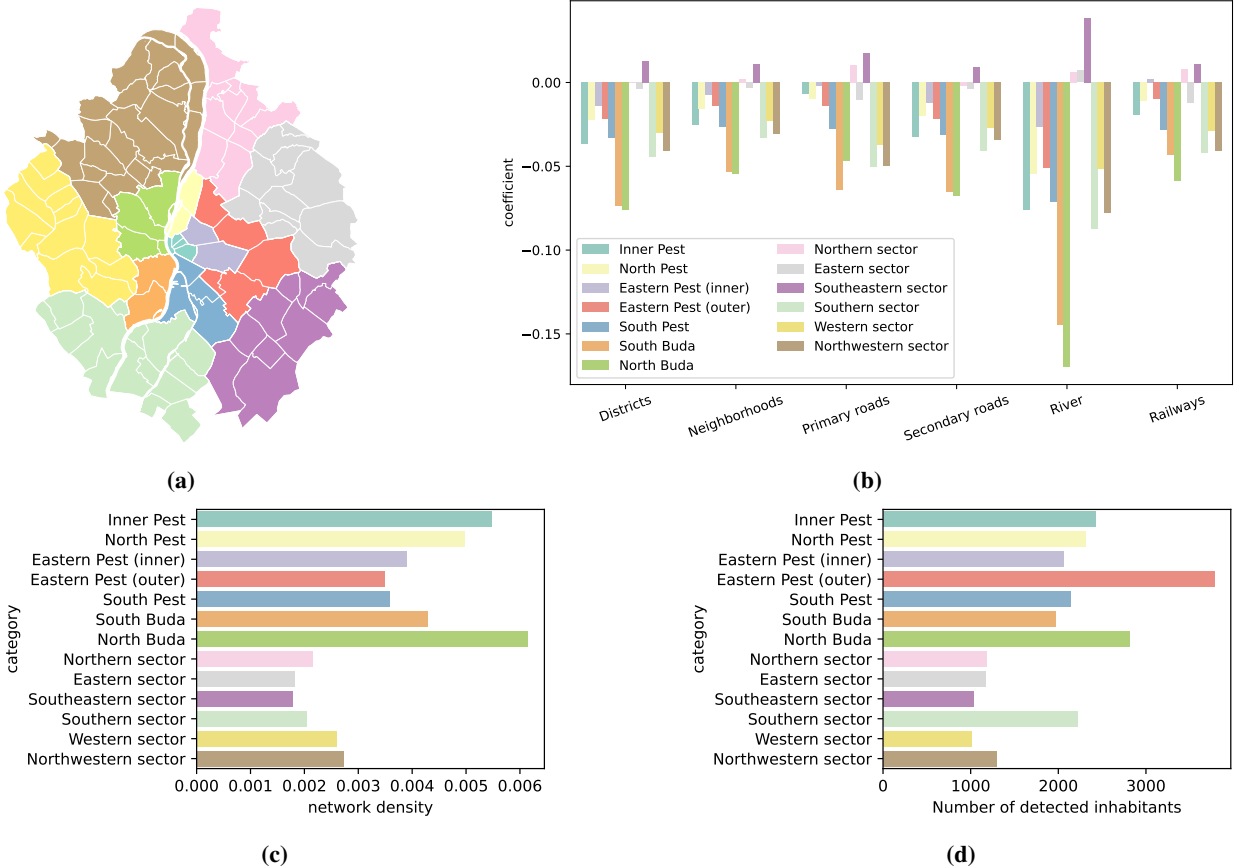


Figure S8: Network details and the barrier effect based on the users' home location groups. The HCSO defines seven district groups in Budapest and six sectors of the agglomeration (a). From the Budapest mobility of the inhabitants of these areas, 13 networks was built and evaluated. Network density shown in c, the detected number of inhabitant in d, and the gravity model coefficients are displayed in b.

S7 Budapest Stops of Inhabitants Living in the Agglomeration

The commuting patterns from the agglomeration sectors to the district groups of Budapest are regularly analyzed by the census data and already studied using mobile network data [4]. Based on the mobile positioning data, utilized in this study, the visitation patterns of Budapest areas from the agglomeration is determined (Figure S9 and Table S1).

Figure S9 shows the distribution of visitations from the agglomeration sectors to the Budapest district groups, using the same colors as in Figure S7a. It is also in numerical format in Table S1, where the rows represent the district groups and the columns represent the agglomeration sectors.

As expected, most of the visit from the eastern sectors target the Pest-side (East of the river) and the city center, while the majority of the visitations from the western sectors trend to the Buda-side (West of the river) and also to the city center.

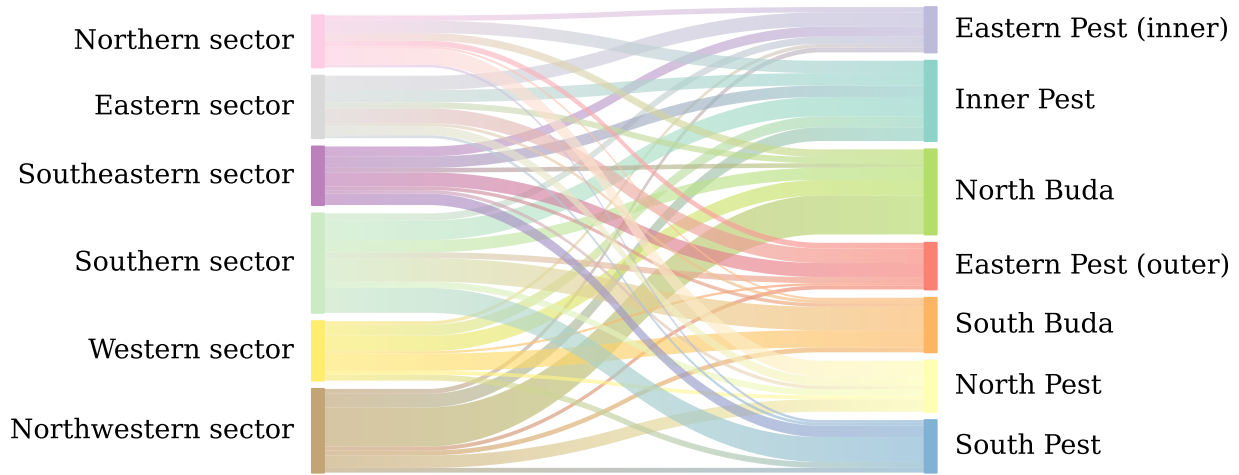


Figure S9: Visitation (stop) distribution within Budapest of the people living in the agglomeration.

Table S1: Stop distribution in the district groups (rows) of inhabitants living in the agglomeration sectors (column).

sector district group	Eastern	Northern	Northwestern	Southeastern	Southern	Western
Eastern Pest (inner)	0.2284	0.1031	0.0579	0.1697	0.0734	0.0609
Eastern Pest (outer)	0.2338	0.1086	0.0478	0.2399	0.0606	0.0395
Inner Pest	0.1978	0.2385	0.1637	0.1959	0.1954	0.1838
North Buda	0.0982	0.1484	0.4664	0.0780	0.1223	0.2606
North Pest	0.1434	0.3093	0.1494	0.0603	0.0634	0.0635
South Buda	0.0508	0.0419	0.0576	0.0616	0.2354	0.2917
South Pest	0.0475	0.0504	0.0571	0.1946	0.2495	0.1000

S8 Aggregated Barrier Crossing Ratio

The Section Barrier Crossing Ratio of the main text introduces the Barrier Crossing Ratio (BCR), which measures the relationship between those mobility events that cross barriers and those that cross barriers and detected communities as well.

Figure S10a shows the change of the BCR changes according to the resolution (γ) during the pre-pandemic interval while Figure S10b shows the same during the pandemic. The two intervals are described in Section S1.

The BCR reaches roughly the same value at higher γ in both cases, however in the pre-pandemic data set that happens faster. This might be the result of the decreased mobility during the pandemic.

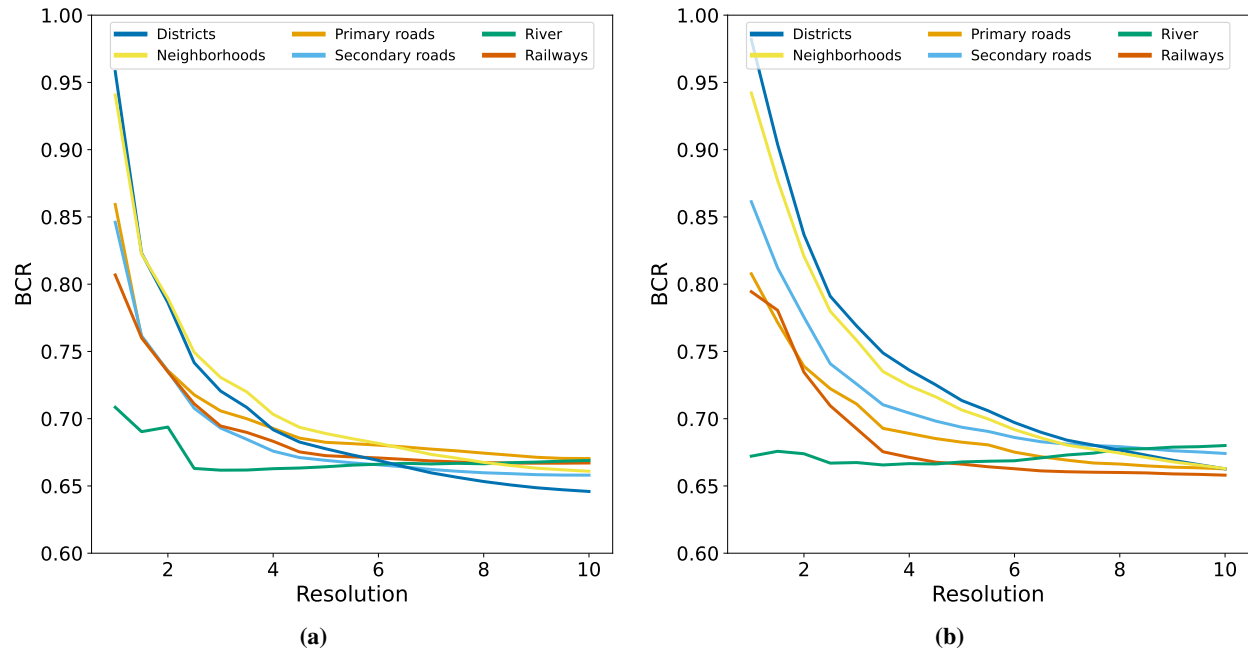


Figure S10: Aggregated Barrier Crossing Ratio (BCR) for the pre-pandemic (a) and the pandemic data sets (b).

S9 Complexity OLS tables

The Barrier Crossing Ratio (BCR) is regressed with an Ordinary Least Squares (OLS) linear regression, using the formula (4) from the main text. The explanatory variables are the geographical distance of the user’s home location from the city center and the complexity of amenity portfolio of the visited location as proposed by [3]. The BCR is explained separately by the barrier types of primary roads (Table S2), secondary roads (Table S3), districts (Table S4), neighborhoods (Table S5), rivers (Table S6), and railways (Table S7), and for increasing resolution (γ) values.

Table S2: Primary roads

dependent variable: $BCR^{Primary\ roads}$										
	$\gamma = 1$	$\gamma = 2$	$\gamma = 3$	$\gamma = 4$	$\gamma = 5$	$\gamma = 6$	$\gamma = 7$	$\gamma = 8$	$\gamma = 9$	$\gamma = 10$
intercept	2.085*** (0.319)	0.669*** (0.184)	-0.009 (0.137)	-0.014 (0.131)	0.089 (0.120)	-0.639 (0.644)	-0.124 (0.202)	0.395*** (0.088)	0.311*** (0.115)	0.419*** (0.087)
distance (log10)	-0.117 (0.084)	0.180*** (0.048)	0.338*** (0.036)	0.329*** (0.035)	0.288*** (0.032)	0.489*** (0.170)	0.337*** (0.053)	0.188*** (0.023)	0.208*** (0.030)	0.177*** (0.023)
complexity	0.150*** (0.027)	-0.137*** (0.016)	-0.094*** (0.012)	-0.097*** (0.011)	-0.077*** (0.010)	-0.081 (0.054)	-0.086*** (0.017)	-0.092*** (0.007)	-0.076*** (0.010)	-0.089*** (0.007)
observations	15697	15957	16126	16263	16343	16418	16472	16500	16521	16549
R ²	0.003	0.007	0.013	0.014	0.012	0.001	0.006	0.018	0.009	0.017
adjusted R ²	0.002	0.007	0.013	0.014	0.012	0.001	0.006	0.018	0.009	0.017

Table S3: Secondary roads

dependent variable: $BCR^{Secondary\ roads}$										
	$\gamma = 1$	$\gamma = 2$	$\gamma = 3$	$\gamma = 4$	$\gamma = 5$	$\gamma = 6$	$\gamma = 7$	$\gamma = 8$	$\gamma = 9$	$\gamma = 10$
intercept	2.358*** (0.237)	1.044*** (0.217)	0.093 (0.199)	-0.029 (0.428)	0.271* (0.143)	0.171 (0.125)	0.137 (0.131)	0.256*** (0.129)	0.300*** (0.102)	0.192* (0.105)
distance (log10)	-0.169*** (0.062)	0.128*** (0.057)	0.345*** (0.052)	0.367*** (0.113)	0.269*** (0.038)	0.287*** (0.033)	0.288*** (0.034)	0.252*** (0.034)	0.236*** (0.027)	0.261*** (0.028)
complexity	-0.087*** (0.020)	-0.224*** (0.018)	-0.142*** (0.017)	-0.188*** (0.036)	-0.150*** (0.012)	-0.156*** (0.010)	-0.143*** (0.011)	-0.156*** (0.011)	-0.151*** (0.009)	-0.143*** (0.009)
observations	15747	15951	16139	16248	16339	16404	16453	16473	16501	16525
R ²	0.001	0.012	0.010	0.003	0.017	0.024	0.020	0.021	0.031	0.029
adjusted R ²	0.001	0.011	0.010	0.003	0.017	0.024	0.020	0.021	0.031	0.028

Table S4: Districts

dependent variable: $BCR^{Districts}$										
	$\gamma = 1$	$\gamma = 2$	$\gamma = 3$	$\gamma = 4$	$\gamma = 5$	$\gamma = 6$	$\gamma = 7$	$\gamma = 8$	$\gamma = 9$	$\gamma = 10$
intercept	3.022*** (0.275)	1.132*** (0.205)	-0.097 (0.170)	0.092 (0.159)	0.191 (0.139)	0.052 (0.133)	-0.007 (0.130)	0.143 (0.114)	0.105 (0.115)	0.065 (0.109)
distance (log10)	-0.225*** (0.072)	0.191*** (0.054)	0.469*** (0.045)	0.395*** (0.042)	0.346*** (0.037)	0.374*** (0.035)	0.378*** (0.034)	0.328*** (0.030)	0.335*** (0.030)	0.339*** (0.029)
complexity	-0.113*** (0.023)	-0.335*** (0.017)	-0.201*** (0.014)	-0.242*** (0.013)	-0.209*** (0.012)	-0.220*** (0.011)	-0.217*** (0.011)	-0.218*** (0.009)	-0.220*** (0.010)	-0.215*** (0.009)
observations	15831	16035	16202	16321	16400	16467	16516	16538	16562	16585
R ²	0.002	0.029	0.026	0.034	0.033	0.041	0.042	0.050	0.050	0.055
adjusted R ²	0.002	0.028	0.026	0.034	0.033	0.040	0.042	0.050	0.050	0.054

Table S5: Neighborhoods

dependent variable: $BCR^{Neighborhoods}$										
	$\gamma = 1$	$\gamma = 2$	$\gamma = 3$	$\gamma = 4$	$\gamma = 5$	$\gamma = 6$	$\gamma = 7$	$\gamma = 8$	$\gamma = 9$	$\gamma = 10$
intercept	1.466*** (0.266)	0.404* (0.219)	-0.522*** (0.182)	-0.209 (0.179)	0.035 (0.161)	-0.071 (0.158)	-0.044 (0.138)	0.201* (0.115)	0.183 (0.118)	0.162 (0.114)
distance (log10)	0.150*** (0.070)	0.359*** (0.058)	0.566*** (0.048)	0.462*** (0.047)	0.376*** (0.042)	0.396*** (0.042)	0.376*** (0.036)	0.301*** (0.030)	0.303*** (0.031)	0.304*** (0.030)
complexity	-0.048*** (0.023)	-0.244*** (0.018)	-0.155*** (0.015)	-0.202*** (0.015)	-0.172*** (0.013)	-0.190*** (0.013)	-0.187*** (0.012)	-0.193*** (0.010)	-0.195*** (0.010)	-0.193*** (0.009)
observations	15831	16035	16202	16321	16400	16467	16516	16538	16562	16585
R ²	0.001	0.018	0.021	0.023	0.020	0.025	0.030	0.040	0.038	0.041
adjusted R ²	0.001	0.018	0.020	0.023	0.020	0.025	0.030	0.039	0.038	0.041

Table S6: River

dependent variable: BCR^{River}										
	$\gamma = 1$	$\gamma = 2$	$\gamma = 3$	$\gamma = 4$	$\gamma = 5$	$\gamma = 6$	$\gamma = 7$	$\gamma = 8$	$\gamma = 9$	$\gamma = 10$
intercept	-0.064 (0.106)	-0.328*** (0.078)	-0.344*** (0.101)	-0.397*** (0.061)	-0.404*** (0.063)	-0.381*** (0.061)	-0.375*** (0.064)	-0.334*** (0.061)	-0.328*** (0.063)	-0.329*** (0.065)
distance (log10)	0.242*** (0.028)	0.299*** (0.021)	0.299*** (0.027)	0.300*** (0.016)	0.300*** (0.017)	0.293*** (0.016)	0.291*** (0.017)	0.280*** (0.016)	0.278*** (0.017)	0.278*** (0.017)
complexity	0.102*** (0.009)	0.092*** (0.007)	0.117*** (0.009)	0.121*** (0.005)	0.127*** (0.005)	0.125*** (0.005)	0.126*** (0.005)	0.126*** (0.005)	0.122*** (0.005)	0.124*** (0.005)
observations	15788	15994	16102	16311	16390	16457	16506	16525	16548	16574
R ²	0.010	0.019	0.015	0.042	0.042	0.044	0.040	0.043	0.038	0.037
adjusted R ²	0.010	0.019	0.015	0.042	0.042	0.043	0.040	0.043	0.037	0.037

Table S7: Railways

dependent variable: $BCR^{Railways}$										
	$\gamma = 1$	$\gamma = 2$	$\gamma = 3$	$\gamma = 4$	$\gamma = 5$	$\gamma = 6$	$\gamma = 7$	$\gamma = 8$	$\gamma = 9$	$\gamma = 10$
intercept	0.004 (0.217)	-0.021 (0.183)	-0.548*** (0.187)	-0.450*** (0.151)	-0.081 (0.121)	-0.175 (0.137)	-0.157* (0.089)	0.345*** (0.076)	0.426*** (0.078)	0.326*** (0.070)
distance (log10)	0.404*** (0.057)	0.376*** (0.048)	0.499*** (0.049)	0.453*** (0.040)	0.334*** (0.032)	0.357*** (0.036)	0.341*** (0.023)	0.199*** (0.020)	0.175*** (0.020)	0.198*** (0.018)
complexity	-0.128*** (0.019)	-0.188*** (0.015)	-0.138*** (0.016)	-0.127*** (0.013)	-0.095*** (0.010)	-0.100*** (0.011)	-0.097*** (0.007)	-0.108*** (0.006)	-0.112*** (0.006)	-0.107*** (0.006)
observations	15697	15923	16117	16259	16347	16428	16465	16506	16536	16559
R ²	0.009	0.018	0.015	0.019	0.017	0.015	0.032	0.031	0.029	0.036
adjusted R ²	0.009	0.018	0.015	0.019	0.017	0.015	0.032	0.031	0.029	0.036

S10 YJMob100K

A metropolitan scale, longitudinal, and anonymized mobility trajectory data was released [5], which aims to be a benchmark dataset of human mobility [6]. The presented approach was applied to the ‘YJMob100K’ data set, which already contains trajectories in their raw form. The exact procedure that made it possible to use the ‘YJMob100K’ data for this study can be found in [7]. The difference is that the trajectories connect 500 meters by 500 meters grid cells, instead of blocks extracted from the road network. Figure S11b and S11c illustrate the results of the community detection procedure at resolution (γ) 1, 5, and 12 in contrast of the municipalities (solid line) and wards (dotted line) extracted from OpenStreetMap (OSM). The mobility clusters match the administrative boundaries, but a community often matches multiple municipalities. Interestingly, this effect does not apply to the road network (Figure S11d, S11e, S11f) as in the case of Budapest (Figure 1 of the main text). Note that the water surfaces are excluded from the municipality boundaries. However, activities occur there (e.g., people using ferries), which can be observed in the data, so some of those cells are associated with communities.

The Symmetric Area Difference (SAD) is calculated (Figure S11g) compared to the municipality boundaries (admin level 7 in OSM) and the wards of Nagoya (admin level 8 in OSM). In both cases, the SAD approximates the administrative boundaries as the resolution increases.

The individual Barrier Crossing Ratio (BCR) is also determined based on the ‘YJMob100K’ data. Similarly to the Budapest case, people with estimated home locations within Nagoya (18,699 individuals) are distinguished from the rest of the users. Just as in the case of Budapest, the two groups show different exposure to the barrier effect (Figure S11h and S11i), however, as opposed to Budapest the relation of the two trends are the opposite.

In this section, we demonstrated our approach on a different data set covering a much larger area from a different part of the world. The ‘YJMob100K’ data set follows 100,000 people in about a 100 km by 100 km area, while Budapest and its agglomeration is about 2540 km². The administrative area of Nagoya as a principal city is 326.45 km², which is about the 62% of Budapest (525.14 km²), however, Nagoya is the center of the Chūkyō metropolitan area with the area of 7072 km². In our study, we focused on mobility that took place within the administrative boundaries of Budapest, a smaller area but with more users. Due to the high number of differences not every result shows exactly the expected finding. Further study is required, involving data about more cities, to explore the barrier effect in more types of cities.

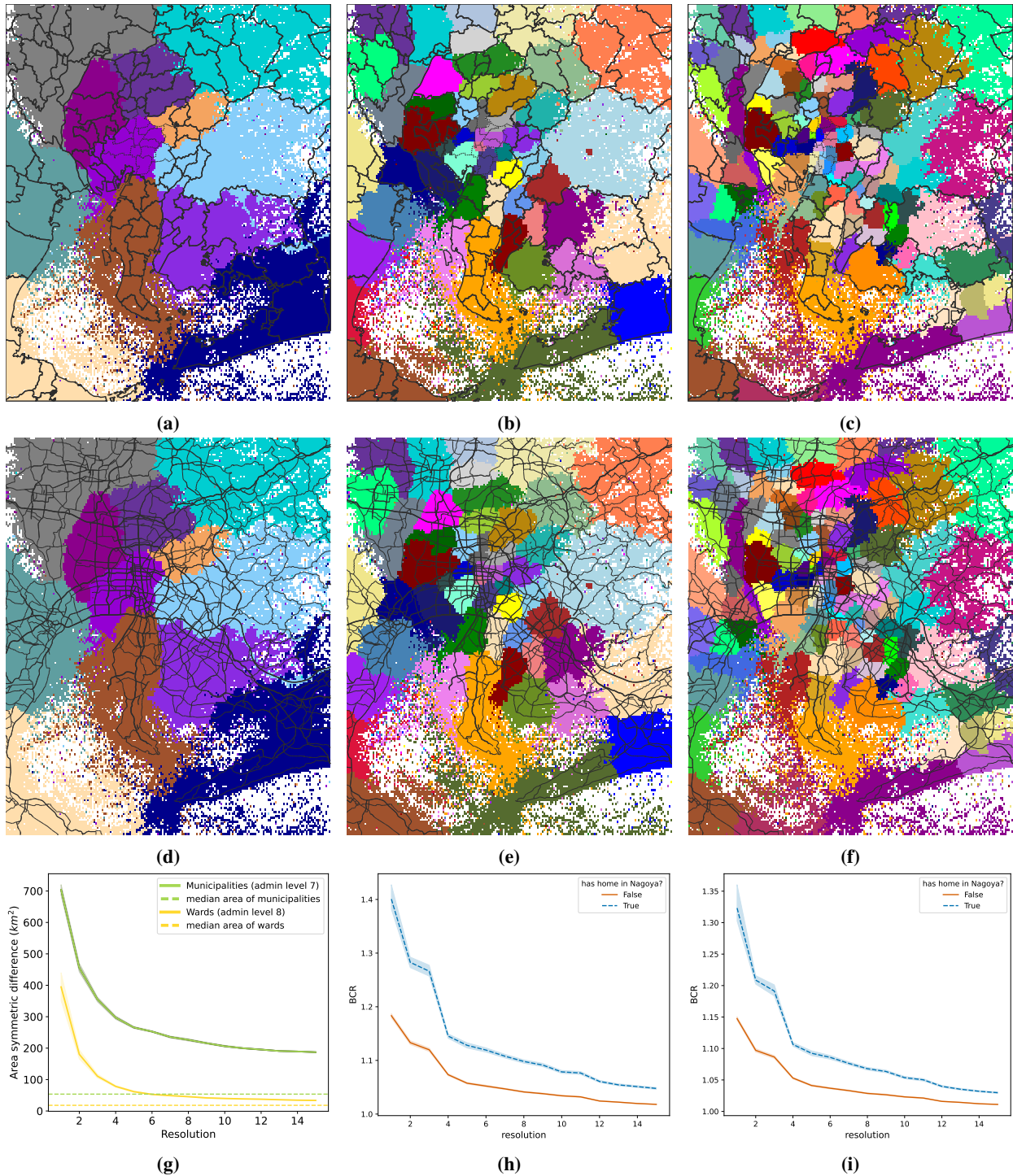


Figure S11: Louvain communities compared to administrative boundaries at resolution 1 (a), 5 (b), and 12 (c), and compared to the road network at resolution 1, 5, and 12 (d, e, and f respectively). The decreasing Symmetric Area Difference shows an improving fit of mobility clusters to the administrative boundaries (g). The individual Barrier Crossing Ratio shows that the barriers like municipality boundaries (h) and primary roads (i) affect people less if they have home locations in Nagoya compared to those who live in its agglomeration.

Abbreviations

- BCR** Barrier Crossing Ratio
GPS Global Positioning System
HCSO Hungarian Central Statistical Office
OLS Ordinary Least Squares
OSM OpenStreetMap
SAD Symmetric Area Difference

Supplementary References

- [1] European Centre for Disease Prevention and Control. *Data on 14-day notification rate of new COVID-19 cases and deaths*. (Online; accessed on 12 December 2023). Nov. 2023. URL: <https://www.ecdc.europa.eu/en/publications-data/data-national-14-day-notification-rate-covid-19> (visited on 11/17/2023).
- [2] Dani Arribas-Bel and Martin Fleischmann. *Generating enclosures (proof of a concept)*. (Online; accessed on 27 July 2023). 2020. URL: https://urbangrammarai.xyz/spatial_signatures/spatial_unit/Parallelized_enclosures.html#generate-enclosures (visited on 07/27/2023).
- [3] Sándor Juhász et al. “Amenity complexity and urban locations of socio-economic mixing”. In: *EPJ Data Science* 12.1 (2023), p. 34.
- [4] Gergő Pintér and Imre Felde. “Commuting Analysis of the Budapest Metropolitan Area Using Mobile Network Data”. In: *ISPRS International Journal of Geo-Information* 11.9 (2022), p. 466.
- [5] Takahiro Yabe et al. “YJMob100K: City-scale and longitudinal dataset of anonymized human mobility trajectories”. In: *Scientific Data* 11.1 (2024), p. 397.
- [6] Takahiro Yabe et al. “Enhancing human mobility research with open and standardized datasets”. In: *Nature Computational Science* (2024), pp. 1–4.
- [7] Gergő Pintér. *Revealing urban area from mobile positioning data*. 2024. arXiv: 2407.18086 [cs.SI]. URL: <https://arxiv.org/abs/2407.18086>.